



Efficient Organic Photovoltaic Cells Based on Thiazolothiazole and Benzodithiophene Copolymers with π -Conjugated Bridges

Junhoo Park,¹ Jong Baek Park,¹ Jong-Woon Ha,¹ Hea Jung Park,¹ In-Nam Kang,²
Do-Hoon Hwang ¹

¹Department of Chemistry and Chemistry Institute for Functional Materials, Pusan National University, Busan, 46241, Republic of Korea

²Department of Chemistry, The Catholic University of Korea, Gyeonggi-do, 420-743, Republic of Korea

Correspondence to: D.-H. Hwang (E-mail: dohoonhwang@pusan.ac.kr)

Received 6 May 2018; accepted 2 June 2018; published online 00 Month 2018

DOI: 10.1002/pola.29084

ABSTRACT: New donor- π -acceptor (D- π -A) type conjugated copolymers, poly[(4,8-bis((2-hexyldecyl)oxy)benzo[1,2-*b*:4,5-*b'*]dithiophene)-*alt*-(2,5-bis(4-octylthiophen-2-yl)thiazolo[5,4-*d*]thiazole)] (PBDT-tTz), and poly[(4,8-bis((2-hexyldecyl)oxy)benzo[1,2-*b*:4,5-*b'*]dithiophene)-*alt*-(2,5-bis(6-octylthieno[3,2-*b*]thiophen-2-yl)thiazolo[5,4-*d*]thiazole)] (PBDT-ttTz) were synthesized and characterized with the aim of investigating their potential applicability to organic photovoltaic active materials. While copolymer PBDT-tTz showed a zigzagged non-linear structure by thiophene π -bridges, PBDT-ttTz had a linear molecular structure with thieno[3,2-*b*]thiophene π -bridges. The optical, electrochemical, morphological, and photovoltaic properties of PBDT-tTz and PBDT-ttTz were systematically investigated. Furthermore, bulk heterojunction photovoltaic devices were fabricated

by using the synthesized polymers as p-type donors and [6,6]-phenyl-C₇₁-butyric acid methyl ester as an n-type acceptor. PBDT-tTz showed a high power conversion efficiency (PCE) of 5.21% as a result of the extended conjugation arising from the thienothiophene π -bridges and enhanced molecular ordering in the film state, while PBDT-ttTz showed a relatively lower PCE of 2.92% under AM 1.5 G illumination (100 mW/cm²). © 2017 Wiley Periodicals, Inc. *J. Polym. Sci., Part A: Polym. Chem.* **2017**, *00*, 000–000

KEYWORDS: thieno[3,2-*b*]thiophene; thiazolo[5,4-*d*]thiazole; benzo[1,2-*b*:4,5-*b'*]dithiophene; wide-band gap polymer; organic photovoltaic cells

INTRODUCTION In recent years, research into high-efficiency organic photovoltaic cells (OPVs) has expanded tremendously and led to the development of various semiconducting materials, especially donor-acceptor (D-A) conjugated polymers, which have achieved high power conversion efficiencies (PCEs) of over 11% when blended with fullerene-derivative acceptors.^{1–4} Conjugated polymers incorporating electron donating and accepting (D-A) systems that exhibit broad absorption in the UV-visible region and possess appropriate low band gaps (<2 eV) and HOMO-LUMO energy levels by the intra-molecular charge transfer (ICT), have particularly attracted a lot of attention.^{5–7}

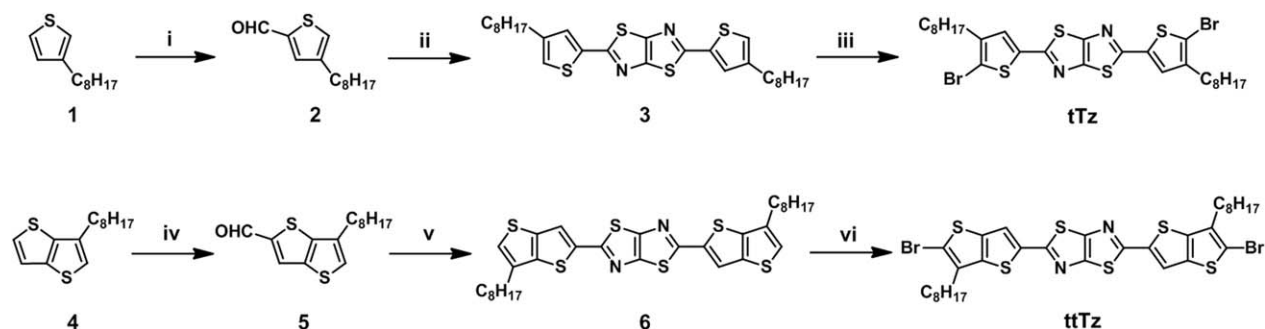
Among the various electron-donating units, benzo[1,2-*b*:4,5-*b'*]dithiophene (BDT) is one of the most well-known building blocks for organic solar cells with high PCE.^{4,8} The rigid planar structure with extended π -conjugation of BDT facilitates charge-carrier mobility and improves the π - π interactions between the polymer chains in the solid state. The HOMO

energy levels of BDT-based conjugated polymers can be finely tuned by introducing different substituents on the central phenyl ring.^{9–11} Recently, conjugated polymers based on thiazolo[5,4-*d*]thiazole (Tz) and various electron-donating repeating units have been developed for polymer solar cell applications.^{12–15} The Tz unit, consisting of an electron-deficient fused heterocyclic ring is a good electron acceptor, and exhibits high charge mobility, planarity, and intermolecular stacking.^{16–19}

In this study, we designed and synthesized two new D- π -A type conjugated copolymers, namely, poly[(4,8-bis((2-hexyldecyl)oxy)benzo[1,2-*b*:4,5-*b'*]dithiophene)-*alt*-(2,5-bis(4-octylthiophen-2-yl)thiazolo[5,4-*d*]thiazole)] (PBDT-tTz), and poly[(4,8-bis((2-hexyldecyl)oxy)benzo[1,2-*b*:4,5-*b'*]dithiophene)-*alt*-(2,5-bis(6-octylthieno[3,2-*b*]thiophen-2-yl)thiazolo[5,4-*d*]thiazole)] (PBDT-ttTz), which consist of the electron-rich BDT and electron-deficient Tz units bridged with either alkyl-substituted thiophene (t) or thieno[3,2-

Additional Supporting Information may be found in the online version of this article.

© 2018 Wiley Periodicals, Inc.



SCHEME 1 Synthetic routes of tTz and ttTz monomers: (i) THF, *n*-BuLi, 1-formylpiperidine, room temperature, 2 h. (ii) Dithiooxamide, DMF, 150 °C, 12 h. (iii) NBS, THF/DMF(1:2), 40 °C, 2 h. (iv) THF, *n*-BuLi, 1-formylpiperidine, room temperature, 2 h. (v) Dithiooxamide, DMF, 150 °C, 12 h. (vi) NBS, DMF, 80 °C, 1.5 h.

b]thiophene (tt). The introduction of π -bridges into the D-A copolymers was expected to have an effect on the molecular ordering and consequently influence the photovoltaic properties of the OPV cells.^{20–22} The synthetic routes and chemical structures of the synthesized polymers are shown in Schemes 1 and 2.

EXPERIMENTAL

Materials

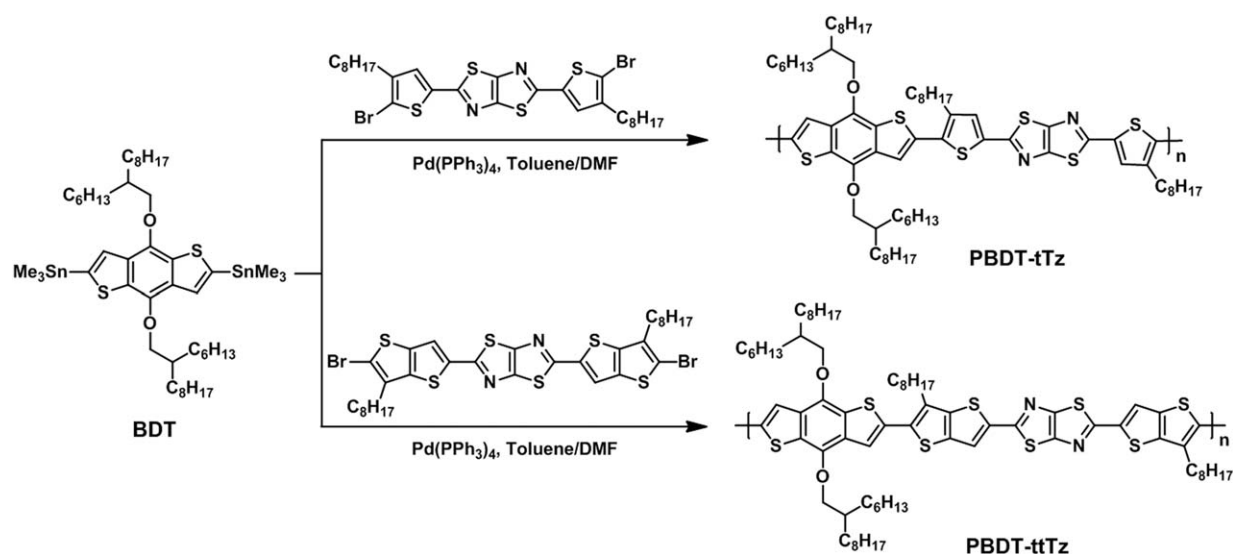
All starting materials and reagents were purchased from Aldrich, Alfa Aesar, and TCI, and used without further purification unless stated otherwise. Tetrakis(triphenylphosphine)palladium(0) ($\text{Pd}(\text{PPh}_3)_4$) catalyst and [6,6]-phenyl-C₇₁-butyric acid methyl ester (PC₇₁BM) were purchased from Strem Chemicals, Inc. and EM-index, respectively. Tetrahydrofuran (THF) was purified by fractional distillation. 3-Octylthiophene (**1**), 3-octylthieno[3,2-*b*]thiophene (**4**), and (4,8-bis((2-hexyldecyl)oxy)benzo[1,2-*b*:4,5-*b'*]dithiophene-2,6-diyl)bis(trimethylstannane) (BDTHD) were synthesized following previously reported procedures.^{23–25}

Characterization

¹H (300 MHz) and ¹³C NMR (75 MHz) spectra were measured using a Varian Mercury Plus spectrometer, and the chemical shifts were recorded in units of parts per million relative to chloroform as the internal standard. The number average molecular weight (M_n) and polydispersity index (PDI) of the polymer was determined by gel permeation chromatography (GPC) analysis relative to a polystyrene standard on an Agilent 1260 Infinity HPLC. The absorption spectra were measured by a JP/UV-1800 UV/Vis spectrophotometer. Cyclic voltammetry (CV) was performed on a CH Instruments Electrochemical Analyzer and the measurements were carried out by using Ag/AgNO₃ as the reference electrode, a platinum wire as the counter electrode, and a platinum wire coated with the synthesized polymer as the working electrode in acetonitrile solution containing 0.1 M tetrabutylammonium tetrafluoroborate (TBABF₄) as the supporting electrolyte.

Synthesis of 4-Octylthiophene-2-Carbaldehyde (**2**)

A vacuum-dried 250 mL flask was charged with compound **1** (8.41 g, 42.83 mmol) and dry THF (100 mL) under Ar



SCHEME 2 Synthetic routes of PBDT-tTz and PBDT-ttTz polymers.

atmosphere. The solution was cooled to -78°C and *n*-BuLi (17.13 mL, 42.83 mmol, 2.5 M solution in hexane) was added slowly to the flask. After 30 min of stirring the reaction mixture at -78°C , 1-formylpiperidine (5.33 g, 47.11 mmol) was added in one portion. The solution was allowed to warm to room temperature and stirred for 2 h. Subsequently, the mixture was poured into water (200 mL) and the organic layer was extracted with ethyl acetate three times. The combined organic layer was washed with brine. After drying over anhydrous MgSO_4 , the solvent was evaporated using a rotary evaporator and the residue was purified by silica gel column chromatography with the solvent mixture of ethyl acetate and hexane (1:6) as the eluent to obtain a yellow oil (5.00 g, 52%). ^1H NMR (300 MHz, CDCl_3 , δ): 9.86 (s, 1H), 7.60 (s, 1H), 7.36 (s, 1H), 2.63 (t, $J = 7.5$ Hz, 2H), 1.67–1.59 (m, 2H), 1.29–1.24 (m, 10H), 0.87 (t, $J = 7.2$ Hz, 3H). ^{13}C NMR (75 MHz, CDCl_3 , δ): 183.0, 144.8, 137.2, 134.4, 130.7, 31.9, 30.4, 29.7, 29.3, 29.2, 28.5, 22.7, 14.1. HRMS (LC/MS): Calcd. for $\text{C}_{13}\text{H}_{20}\text{OS}$, 224.36; Found $[\text{M} + \text{H}]^+$ 225.13. Elem. Anal. Calcd. for $\text{C}_{13}\text{H}_{20}\text{OS}$: C, 69.6; H, 9.0; O, 7.1; S, 14.3; Found, C, 69.6; H, 9.3; O, 8.4; S, 13.2. FTIR (KBr, neat, cm^{-1}): 3096 (sp^2 C–H stretch, m), 2961, 2923 (sp^3 C–H stretch, w), 2853, 2694 (aldehyde C–H stretch, w), 1673 (conjugated C=O stretch, s), 1467 (aromatic C=C stretch, m), 1434, 1239, 1188.

Synthesis of 2,5-Bis(4-Octylthiophen-2-yl)Thiazolo[5,4-d]Thiazole (3)

Dithiooxamide (1.07 g, 8.91 mmol) was added into a solution of compound 2 (5.00 g, 22.29 mmol) dissolved in *N,N*-dimethylformamide (DMF) (80 mL) under N_2 atmosphere. The mixture was stirred overnight at 150°C . Subsequently, the solution was cooled, poured into water (100 mL), and extracted with methylene chloride (3×100 mL). The organic extracts were combined and washed with brine (3×100 mL). After drying over anhydrous MgSO_4 , the solvent was evaporated using a rotary evaporator and the residue was purified by silica gel chromatography using the solvent mixture of methylene chloride and hexane (1:2) as the eluent to obtain a yellow solid (3.55 g, 30%). ^1H NMR (300 MHz, CDCl_3 , δ): 7.41 (s, 2H), 7.05 (s, 2H), 2.62 (t, $J = 7.5$ Hz, 4H), 1.64–1.57 (m, 4H), 1.35–1.25 (m, 20H), 0.87 (t, $J = 7.2$ Hz, 6H). ^{13}C NMR (75 MHz, CDCl_3 , δ): 162.7, 149.6, 144.5, 137.1, 128.0, 123.5, 31.9, 30.4, 30.4, 29.4, 29.2, 22.7, 14.1. HRMS (MALDI-TOF): Calcd. for $\text{C}_{28}\text{H}_{38}\text{N}_2\text{S}_4$, 530.87; Found, 531.18. Elem. Anal. Calcd. for $\text{C}_{28}\text{H}_{38}\text{N}_2\text{S}_4$: C, 63.4; H, 7.2; N, 5.3; S, 24.2; Found, C, 63.8; H, 7.3; N, 5.1; S, 24.5. Melting point = 93°C (760 mmHg). FTIR (KBr, neat, cm^{-1}): 3053 (sp^2 C–H stretch, w), 2960, 2921, 2850 (sp^3 C–H stretch, m), 1486 (aromatic C=C stretch, m), 1380, 1310, 1189.

Synthesis of 2,5-Bis(5-Bromo-4-Octylthiophen-2-yl)Thiazolo[5,4-d]Thiazole (tTz)

N-Bromosuccinimide (NBS, 0.86 g, 4.83 mmol) was added to a solution of compound 3 (1.17 g, 2.20 mmol) in THF/DMF (1:2) (60 mL) and the mixture was stirred at 40°C for 2 h. Subsequently, water was added to the reaction mixture and

the flask contents were transferred to a separatory funnel. The organic layer was washed with water (3×100 mL) and dried over anhydrous MgSO_4 . The solvent was evaporated using a rotary evaporator, and the residue was purified by reprecipitation from methylene chloride and methanol to obtain a yellow solid (0.91 g, 60%). ^1H NMR (300 MHz, CDCl_3 , δ): 7.25 (s, 2H), 2.57 (t, $J = 7.5$ Hz, 4H), 1.62–1.59 (m, 4H), 1.33–1.28 (m, 20H), 0.88 (t, $J = 6.9$ Hz, 6H). ^{13}C NMR (75 MHz, CDCl_3 , δ): 161.8, 149.7, 143.5, 136.7, 127.3, 113.4, 31.9, 29.6, 29.6, 29.5, 29.3, 29.2, 22.7, 14.2. HRMS (MALDI-TOF): Calcd. for $\text{C}_{28}\text{H}_{36}\text{Br}_2\text{N}_2\text{S}_4$, 688.67; Found, 689.03. Elem. Anal. Calcd. for $\text{C}_{28}\text{H}_{36}\text{Br}_2\text{N}_2\text{S}_4$: C, 48.83; H, 5.27; N, 4.07; S, 18.62; Found, C, 49.05; H, 5.13; N, 3.98; S, 18.57. Melting point = 104°C (760 mmHg). FTIR (KBr, neat, cm^{-1}): 3055 (sp^2 C–H stretch, w), 2952, 2922, 2847 (sp^3 C–H stretch, m), 1475 (aromatic C=C stretch, s), 1392, 1291, 1182, 629 (C–Br stretch, s).

Synthesis of 6-Octylthieno[3,2-*b*]Thiophene-2-Carbaldehyde (5)

A vacuum-dried 250 mL flask was charged with compound 4 (3.69 g, 14.62 mmol) and dry THF (80 mL) under Ar atmosphere. The solution was cooled to -78°C and 2.5 M solution of *n*-BuLi in hexane (5.85 mL, 14.62 mmol) was slowly added into the flask. After stirring the mixture at -78°C for 20 min, 1-formylpiperidine (1.98 g, 17.54 mmol) was added in one portion. The solution was allowed to slowly warm to room temperature and then stirred for 2 h. The reaction mixture was subsequently poured into water and extracted with ethyl acetate (3×100 mL). After drying over anhydrous MgSO_4 , the solvent was removed and the crude product was purified by silica gel chromatography using the solvent mixture of methylene chloride and hexane (1:2) as the eluent to obtain an orange oil (3.68 g, 90%). ^1H NMR (300 MHz, CDCl_3 , δ): 9.94 (s, 1H), 7.90 (s, 1H), 7.30 (s, 1H), 2.73 (t, $J = 7.5$ Hz, 2H), 1.77–1.72 (m, 2H), 1.32–1.27 (m, 10H), 0.87 (t, $J = 6.6$ Hz, 3H). ^{13}C NMR (75 MHz, CDCl_3 , δ): 183.5, 146.3, 144.7, 138.6, 135.5, 129.7, 128.5, 31.8, 29.6, 29.4, 29.3, 29.2, 28.4, 22.7, 14.1. HRMS (LC/MS): Calcd. for $\text{C}_{15}\text{H}_{20}\text{OS}_2$, 280.45; Found $[\text{M} + \text{H}]^+$ 281.10. Elem. Anal. Calcd. for $\text{C}_{15}\text{H}_{20}\text{OS}_2$: C, 64.2; H, 7.2; O, 5.7; S, 22.9; Found, C, 64.8; H, 7.2; O, 7.0; S, 22.9. FTIR (KBr, neat, cm^{-1}): 3086 (sp^2 C–H stretch, m), 2959 (sp^3 C–H stretch, m), 2852, 2736 (aldehyde C–H stretch, w), 1668 (conjugated C=O stretch, s), 1464 (aromatic C=C stretch, w), 1416, 1379, 1227, 1176.

Synthesis of 2,5-Bis(6-Octylthieno[3,2-*b*]Thiophen-2-yl)Thiazolo[5,4-*d*]Thiazole (6)

Dithiooxamide (0.72 g, 5.96 mmol) was added to a solution of compound 5 (3.68 g, 13.12 mmol) in DMF (30 mL) under N_2 atmosphere. The mixture was stirred overnight at 150°C and subsequently cooled, poured into water (100 mL), and extracted with methylene chloride (3×100 mL). The organic extracts were combined and washed with brine (3×100 mL). After drying over anhydrous MgSO_4 , the solvent was removed, and the residue was purified by silica gel chromatography (methylene chloride:hexane = 1:2) to

obtain an orange solid (3.37 g, 40%). ^1H NMR (300 MHz, CDCl_3 , δ): 7.74 (s, 2H), 7.11 (s, 2H), 2.75 (t, $J = 6.9$ Hz, 4H), 1.80–1.77 (m, 4H), 1.34–1.28 (m, 20H), 0.88 (t, $J = 7.2$ Hz, 6H). ^{13}C NMR (75 MHz, CDCl_3 , δ): 162.7, 149.8, 141.5, 139.0, 138.1, 135.2, 124.5, 119.4, 31.9, 29.8, 29.4, 29.2, 28.5, 22.7, 14.1. HRMS (MALDI-TOF): Calcd. for $\text{C}_{32}\text{H}_{38}\text{N}_2\text{S}_6$, 643.05; Found, 643.36. Elem. Anal. Calcd. for $\text{C}_{32}\text{H}_{38}\text{N}_2\text{S}_6$: C, 59.8; H, 6.0; N, 4.4; S, 29.9; Found, C, 59.8; H, 6.0; N, 4.2; S, 30.5. Melting point = 168 °C (760 mmHg). FTIR (KBr, neat, cm^{-1}): 3102 (sp^2 C–H stretch, w), 2923, 2848 (sp^3 C–H stretch, w), 1464 (aromatic C=C stretch, m), 1438, 1406, 1297, 1155.

Synthesis of 2,5-Bis(5-Bromo-6-Octylthieno[3,2-*b*]Thiophen-2-yl)Thiazolo[5,4-*d*]Thiazole (ttTz)

N-Bromosuccinimide (0.76 g, 4.27 mmol) was slowly added into a stirred solution of compound **6** (1.24 g, 1.93 mmol) in DMF (30 mL). The mixture was heated at 80 °C for 1.5 h and then cooled to room temperature. The reaction was quenched with water and the flask contents were transferred to a separatory funnel. The organic layer was extracted with chloroform (3×100 mL) and then washed with distilled water (3×100 mL). After drying over anhydrous MgSO_4 , the solvent was evaporated. The residue was then purified by reprecipitation from methylene chloride and methanol to obtain an orange solid (0.69 g, 45%). ^1H NMR (300 MHz, CDCl_3 , δ): 7.65 (s, 2H), 2.76 (t, $J = 7.8$ Hz, 4H), 1.75–1.72 (m, 4H), 1.36–1.28 (m, 20H), 0.89 (t, $J = 6.3$ Hz, 6H). ^{13}C NMR (125 MHz, C_6D_6 , δ): 162.2, 150.3, 140.1, 137.9, 137.4, 136.9, 134.6, 119.0, 113.1, 31.8, 29.2, 28.8, 28.4, 27.8, 22.6, 13.9. HRMS (MALDI-TOF): Calcd. for $\text{C}_{32}\text{H}_{36}\text{Br}_2\text{N}_2\text{S}_6$, 800.84; Found, 801.16. Elem. Anal. Calcd. for $\text{C}_{32}\text{H}_{36}\text{Br}_2\text{N}_2\text{S}_6$: C, 47.99; H, 4.53; N, 3.50; S, 24.02; Found, C, 48.55; H, 4.56; N, 3.46; S, 24.28. Melting point = 233 °C (760 mmHg). FTIR (KBr, neat, cm^{-1}): 3086 (sp^2 C–H stretch, w), 2953, 2922, 2852 (sp^3 C–H stretch, s), 1524, 1405 (aromatic C=C stretch, s), 1296, 1156, 611 (C–Br stretch, m).

Polymerization Procedure

The two polymers were synthesized by palladium-catalyzed Stille coupling polymerization. To a mixture of tTz or ttTz, precursor BDTHD, $\text{Pd}(\text{PPh}_3)_4$ catalyst, anhydrous toluene (10 mL), and anhydrous DMF (1 mL) were added under Ar atmosphere and stirred at 110 °C for 1 day. A small amount of 2-bromothiophene was added as an end-capper into the mixture. After stirring for 2 h, a small amount of 2-(tributylstannyl)thiophene was added as an end-capper into the mixture. The reaction mixture was stirred for an additional 2 h and then poured into methanol (200 mL). The crude polymers were filtered and purified successively by Soxhlet extraction with acetone, hexane, methanol, and chlorobenzene for 12 h. After collecting the filtrate dissolved in chlorobenzene, the reprecipitation process was again performed with chlorobenzene and methanol.

Polymerization of Poly[(4,8-Bis((2-Hexyldecyl)Oxy)Benzo[1,2-*b*:4,5-*B'*]Dithiophene)-Alt-(2,5-Bis(4-Octylthiophen-2-yl)Thiazolo[5,4-*d*]Thiazole)] (PBDT-tTz)

BDTHD (130.0 mg, 0.13 mmol), tTz (89.82 mg, 0.13 mmol), and $\text{Pd}(\text{PPh}_3)_4$ (4.52 mg, 3.91 μmol) were mixed together. The polymer was obtained as a dark-red solid (141 mg, 90%). $M_n = 49$ kg/mol, PDI = 1.8, $T_d = 327$ °C.

Polymerization of Poly[(4,8-Bis((2-Hexyldecyl)Oxy)Benzo[1,2-*b*:4,5-*B'*]Dithiophene)-Alt-(2,5-Bis(6-Octylthieno[3,2-*b*]Thiophen-2-yl)Thiazolo[5,4-*d*]Thiazole)] (PBDT-ttTz)

BDTHD (130.0 mg, 0.13 mmol), ttTz (104.5 mg, 0.13 mmol), and $\text{Pd}(\text{PPh}_3)_4$ (4.52 mg, 3.91 μmol) were mixed together. The polymer was obtained as a dark-green solid (161 mg, 94%). $M_n = 21$ kg/mol, PDI = 1.5, $T_d = 323$ °C.

Fabrication of Organic Photovoltaic Devices

The bulk heterojunction (BHJ) OPV devices were fabricated with the indium tin oxide (ITO)/ZnO/active layer/ MoO_3 /Ag inverted structure. ITO substrate was ultrasonically washed in sequence with detergent, distilled water, acetone, and isopropyl alcohol. It was then treated with UV-ozone plasma for 20 min. The ZnO layer was spin-coated on ITO glass at a speed of 2000 rpm for 30 s. The substrate was then baked at 200 °C for 60 min in air to obtain a thin film with a thickness of 30 nm. The active layer materials with various polymer:PC₇₁BM blend ratios (1.0:1.0, 1.0:1.5, 1.0:2.0, and 1.0:3.0, w/w) were first fully dissolved in chlorobenzene solution (30 mg/mL, active area of 0.09 cm^2). Then, the active layer was spin-coated on the ZnO layer at a speed of 700–1600 rpm for 30 s in a N_2 -filled glove box. After drying for 1 h, the MoO_3 layer (8 nm) and Ag metal anode (100 nm) were deposited by vacuum evaporation at pressures below 3×10^{-6} Torr.

Mobility Measurements

The hole mobilities of the polymers were measured by applying the space-charge limited current (SCLC) model to J - V measurements of the devices with ITO/PEDOT:PSS/active layer/ MoO_3 /Ag configuration. The ITO substrate was washed in sequence with detergent, distilled water, acetone, and isopropyl alcohol and then treated with UV-ozone plasma for 20 min. The PEDOT:PSS (Clevios P Al 4083) was spin-coated on the ITO substrate at a speed of 2000 rpm for 30 s and baked at 150 °C for 15 min to obtain a thin film with a thickness of 40 nm. After baking, the active layer materials were fully dissolved in chlorobenzene solution and spin-coated on the PEDOT:PSS layer at a speed of 700–1300 rpm for 30 s. The substrate was dried for 1 h, and then MoO_3 (8 nm) and Ag (100 nm) cathode were finally coated by vacuum evaporation at a pressure below 3×10^{-6} Torr.

The hole mobilities were calculated from the SCLC model using the Mott–Gurney equation.²⁶

TABLE 1 Molecular and thermal properties of polymers

Polymer	M_n (kg/mol)	M_w (kg/mol)	PDI	T_d^a (°C)	T_g^b (°C)	T_c^b (°C)
PBDT-tTz	49	90	1.8	327	–	–
PBDT-ttTz	21	31	1.5	323	70	240

^a 5% weight loss temperature with a heating rate of 10 °C/min at N₂ atmosphere.

^b Measured by differential scanning calorimetry (DSC) within the range of –20 to 300 °C.

$$J_{\text{SCLC}} = (9/8)\epsilon_r\epsilon_0\mu(V^2/L^3)$$

where, ϵ_r is the dielectric constant, ϵ_0 refers to vacuum permittivity (8.85×10^{-14} C/V·cm), μ stands for hole mobility, $V = V_{\text{appl}} - V_{\text{bi}}$ (V_{appl} is the applied potential, V_{bi} is the built-in voltage that results from the difference in the work functions of the cathode and anode), and L refers to the film thickness. The J - V curves of the hole-only devices and field-dependent hole mobilities in the SCLC regime are shown in Supporting Information Figure S4.

Two-Dimensional (2D) Grazing-Incidence X-Ray Diffraction (GIXD) Analysis

The 2D grazing-incidence X-ray diffraction (GIXD) measurements were performed at the 3C beamline in the Pohang Accelerator Laboratory, South Korea. To obtain information about the crystallinity of materials in the solid thin film state, the materials were spin-coated on the ZnO-modified Si wafer (15 × 15 mm) under the same conditions as those used for the OPV device fabrication. The X-ray wavelength was 1.290 Å and the incidence angle (the angle between the irradiation beam and the Si wafer) was 0.12°. The crystallinity of the materials was decoded using a 2D CCD detector (Rayonix SX165), and the X-ray irradiation time was fixed at 30 s. The results obtained from the detector were analyzed according to the relationship between the scattering vector q and the d spacing, $q = 2\pi/d$.

RESULTS AND DISCUSSION

Synthesis and Characterization of PBDT-tTz and PBDT-ttTz

The two polymers, PBDT-tTz and PBDT-ttTz, were synthesized by Stille coupling polymerization using Pd(PPh₃)₄ as a catalyst in anhydrous toluene/DMF (10/1, v/v) solution. The detailed synthetic procedures are described in the Experimental section. PBDT-tTz and PBDT-ttTz were found to be soluble in common organic solvents such as chlorobenzene, *o*-dichlorobenzene, and hot chloroform. The M_n and PDI of the synthesized polymers PBDT-tTz and PBDT-ttTz were measured by gel permeation chromatography (GPC) using chloroform as an eluent at 35 °C and found to be 49,000 and 21,000 g/mol, and 1.8 and 1.5, respectively (Table 1). The thermal properties of the two polymers were investigated by thermogravimetric analysis (TGA) and differential scanning

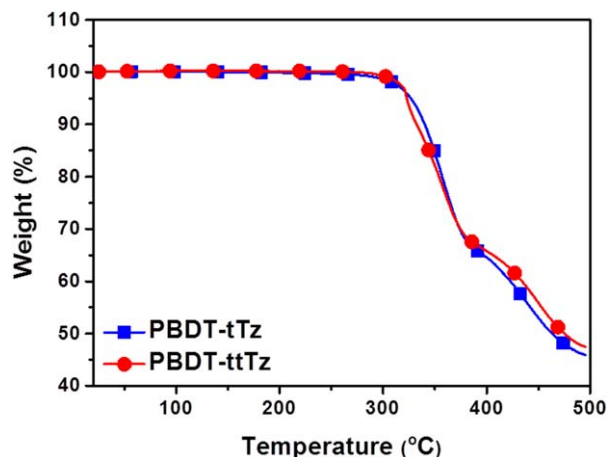


FIGURE 1 TGA curves of the synthesized polymers with a heating rate of 10 °C/min under N₂ atmosphere. Heating range was 20–500 °C. [Color figure can be viewed at wileyonlinelibrary.com]

calorimetry (DSC). The thermal decomposition temperatures (T_d , 5% weight loss temperature) of PBDT-tTz and PBDT-ttTz were 327 and 323 °C, respectively (Fig. 1 and Table 1). There

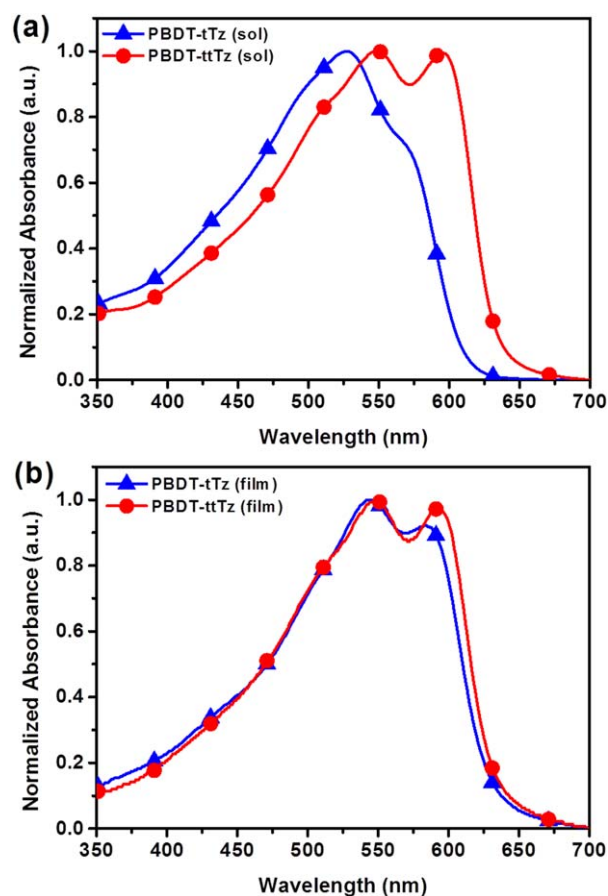


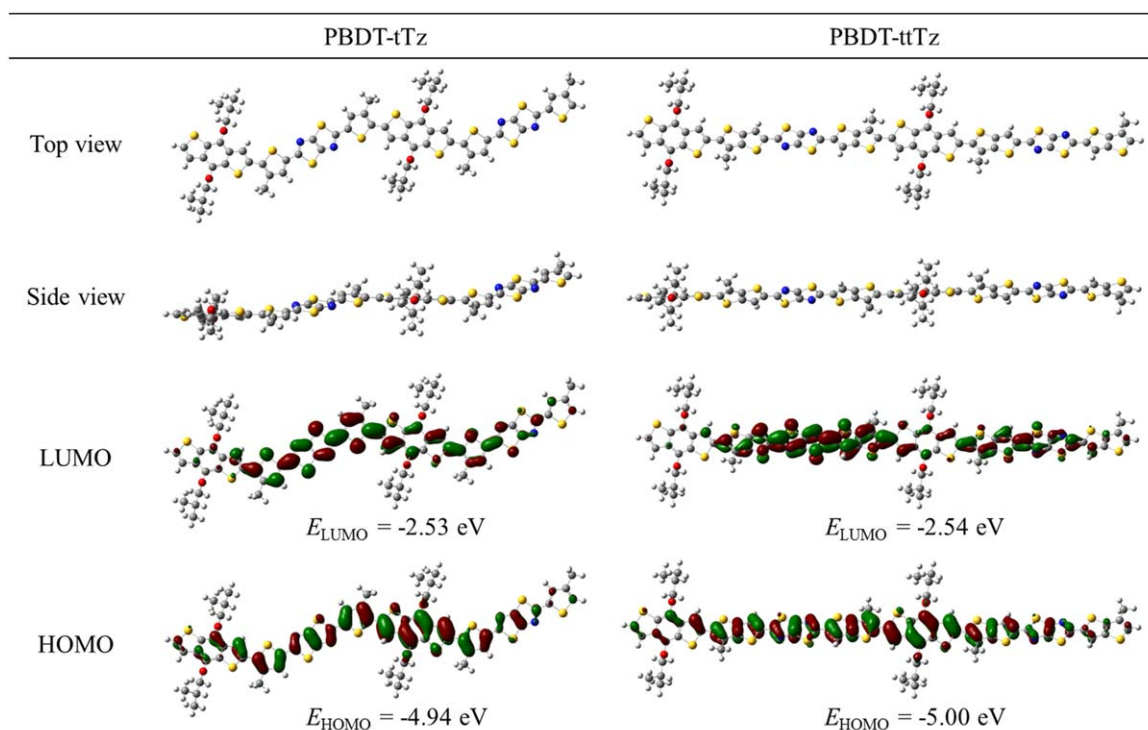
FIGURE 2 UV-vis absorption spectra of PBDT-tTz and PBDT-ttTz (a) in chlorobenzene solution and (b) thin film state. [Color figure can be viewed at wileyonlinelibrary.com]

TABLE 2 Optical and electrochemical properties of the polymers

Polymer	Solution λ_{\max} (nm)	Film λ_{\max} (nm)	E_g^{opt} (eV) ^a	E_{ox} (eV)	E_{HOMO} (eV) ^b	E_{LUMO} (eV) ^c
PBDT-tTz	527, 570	544, 584	1.97	0.65	-5.35	-3.38
PBDT-ttTz	549, 595	549, 595	1.96	0.58	-5.28	-3.32

^a Calculated from the absorption λ_{edge} of polymer films: $E_g^{\text{opt}} = 1240/\lambda_{\text{edge}}$.

^b $E_{\text{HOMO}} = -(4.7 + E_{\text{ox}})$.
^c $E_{\text{LUMO}} = E_g^{\text{opt}} + E_{\text{HOMO}}$.

**FIGURE 3** Top views, side views, and HOMO and LUMO orbitals of two repeating groups of polymers with minimum alkyl chains calculated by DFT using the B3LYP, 6-31G(d). [Color figure can be viewed at wileyonlinelibrary.com]

was no significant difference in the thermal stabilities of PBDT-tTz and PBDT-ttTz. Furthermore, the TGA data of PBDT-tTz and PBDT-ttTz indicated that these polymers are suitable for the fabrication of polymer solar cell devices.²⁶ PBDT-ttTz exhibited a glass transition temperature (T_g) at 70 °C and a crystallization temperature (T_c) at 240 °C,

whereas PBDT-tTz showed no detectable peaks in the DSC thermogram (Supporting Information Fig. S1).

Optical and Electrochemical Properties

The UV-Visible absorption spectra of the two polymers in chlorobenzene solution and thin solid film states are shown

TABLE 3 Best photovoltaic performances and hole mobilities of the OPV devices based on polymer:PC₇₁BM 1.0:2.0 and 1.0:2.0 with 1 vol % 1-CN under AM 1.5G illumination, 100 mW/cm²

Polymer	Additive	V_{OC} (V) ^a	J_{SC} (mA/cm ²) ^a	FF (%) ^a	PCE_{max} (avg) (%) ^a	μ_{h} (cm ² /Vs) ^b
PBDT-tTz	Without	0.73	4.40 [3.96] ^c	46.5	1.50 (1.35)	2.21×10^{-4}
	With	0.76	6.09 [5.85] ^c	63.1	2.92 (2.66)	5.04×10^{-4}
PBDT-ttTz	Without	0.79	10.15 [9.89] ^c	64.8	5.21 (5.14)	9.61×10^{-4}
	With	0.81	8.49 [8.18] ^c	58.2	3.99 (3.89)	7.07×10^{-4}

^a Photovoltaic properties of the polymer:PC₇₁BM devices spin-coated from chlorobenzene solution. The devices consist of ITO/ZnO/active layer/MoO₃/Ag.

^b Measured by applying the SCLC model. The devices consist of ITO/PEDOT:PSS/active layer/MoO₃/Ag.

^c J_{SC} value calculated by EQE.

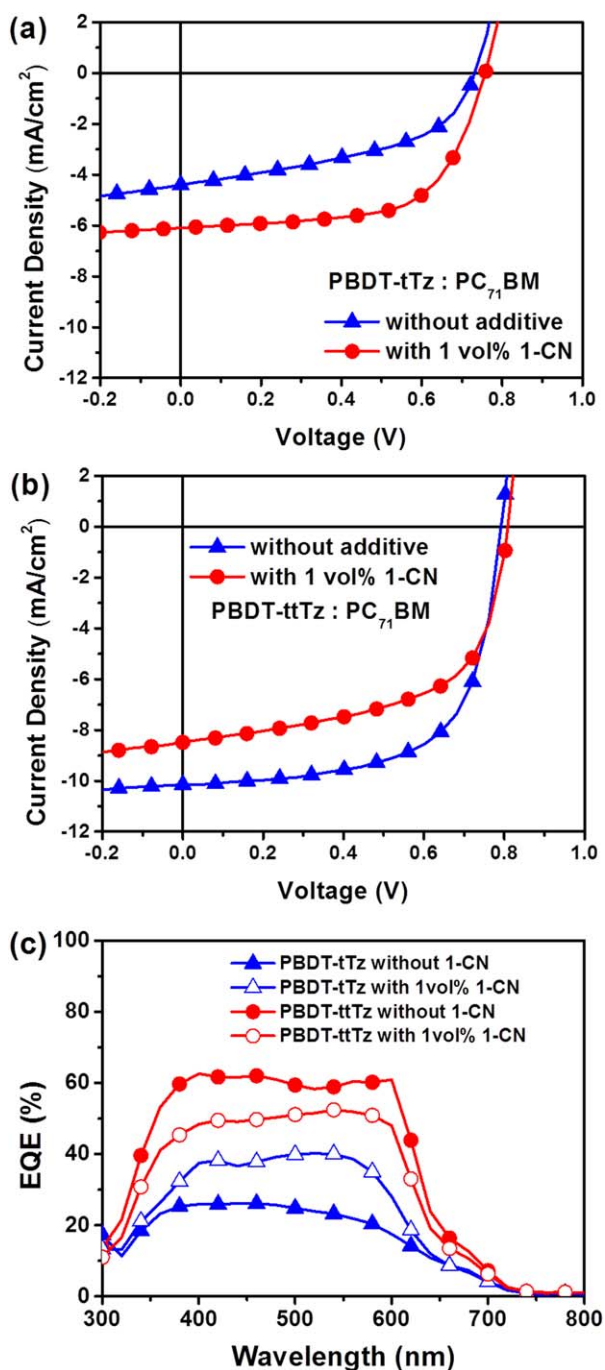


FIGURE 4 *J*-*V* curves of (a) PBDT-tTz:PC₇₁BM (1.0:2.0) and (b) PBDT-ttTz:PC₇₁BM (1.0:2.0) blend films with or without the additive (1 vol % 1-CN) measured under AM 1.5G illumination, 100 mW/cm²; (c) EQE curves of the OPV devices. [Color figure can be viewed at wileyonlinelibrary.com]

in Figure 2. The maximum absorption peaks (λ_{\max}) of the polymers in chlorobenzene solution were observed at 527 and 549 nm for PBDT-tTz and PBDT-ttTz, respectively (Table 2). The absorption maximum of PBDT-ttTz was shifted by 22 nm toward the longer wavelength region than that of PBDT-tTz in solution because of greater extended π -

conjugation of polymer backbone. Additionally, owing to the strong intermolecular interaction by enhanced π - π stacking in the solid state, the PBDT-ttTz film exhibited an increase in the absorption shoulder at 595 nm. In the film state, PBDT-tTz exhibited absorption λ_{\max} at 544 nm, which was red-shifted by 17 nm compared with the peak in the solution spectrum. This was attributed to the enhanced π - π stacking in the solid state.²⁷ Interestingly, the positions of the absorption peaks of PBDT-tTz film (i.e., 549 and 595 nm) were the same as those of the polymer solution. This suggested that the thieno[3,2-*b*]thiophene bridge in the polymer backbone enhanced the π -stacking between the polymer chains even in the solution state. For detailed structural information of the polymers, density functional theory (DFT) calculations were performed. The optical energy band gaps (E_g^{opt}) of the PBDT-tTz and PBDT-ttTz polymer thin films were measured from their onset absorption wavelengths and determined to be 1.97 and 1.96 eV, respectively.

The HOMO energy levels (E_{HOMO}) of the synthesized polymers were measured by cyclic voltammetry (CV) with a platinum wire as a counter electrode and Ag/Ag⁺ as a reference electrode in anhydrous acetonitrile with 0.1 M TBABF₄ as the supporting electrolyte at a scan rate of 50 mV/s.

The CV curves of polymers are shown in Supporting Information Figure S2. E_{HOMO} levels were determined to be -5.35 and -5.28 eV for PBDT-tTz and PBDT-ttTz, respectively, by the following equation, $E_{\text{HOMO}} = -(E_{\text{ox}}^{\text{onset}} + 4.70)$ (eV). The E_{HOMO} of PBDT-ttTz was slightly higher than that of PBDT-tTz because the thieno[3,2-*b*]thiophene group has a stronger electron-donating ability than the thiophene group.²⁸ The LUMO energy levels (E_{LUMO}) were determined to be -3.38 and -3.32 eV for PBDT-tTz and PBDT-ttTz, respectively, by the following equation, $E_{\text{LUMO}} = E_g^{\text{opt}} + E_{\text{HOMO}}$ (eV). The E_{LUMO} levels of the two synthesized polymers were higher than that of PC₇₁BM (ca., -4.30 eV), which is very promising for their application in BHJ OPV cells as donor materials.²⁹ The optical and electrochemical properties of the polymers are summarized in Table 2.

Density Functional Theory (DFT) Calculations

DFT calculations were carried out to gain a deeper understanding of the electronic distributions of the polymers using the Gaussian 09W program with B3LYP functional and 6-31G(d) basis sets. The calculations were performed on two repeating groups and minimum alkyl chains (methyl, isobutyl) to reduce excessive computation demand. While these simple model calculations sometimes fail to capture the important physical characteristics of polymers, they can still provide useful information about the trends in electronic properties.²⁴ The optimized geometries and the HOMO and LUMO orbitals of the two repeating groups of the backbones of PBDT-tTz and PBDT-ttTz are shown in Figure 3. PBDT-tTz demonstrates a zigzagged non-planar geometry with the thiophene π -bridge acting as a bent and twisted connector in the polymer backbone. The steric hindrance between the substituted alkyl chain on the 4-position of the thiophene

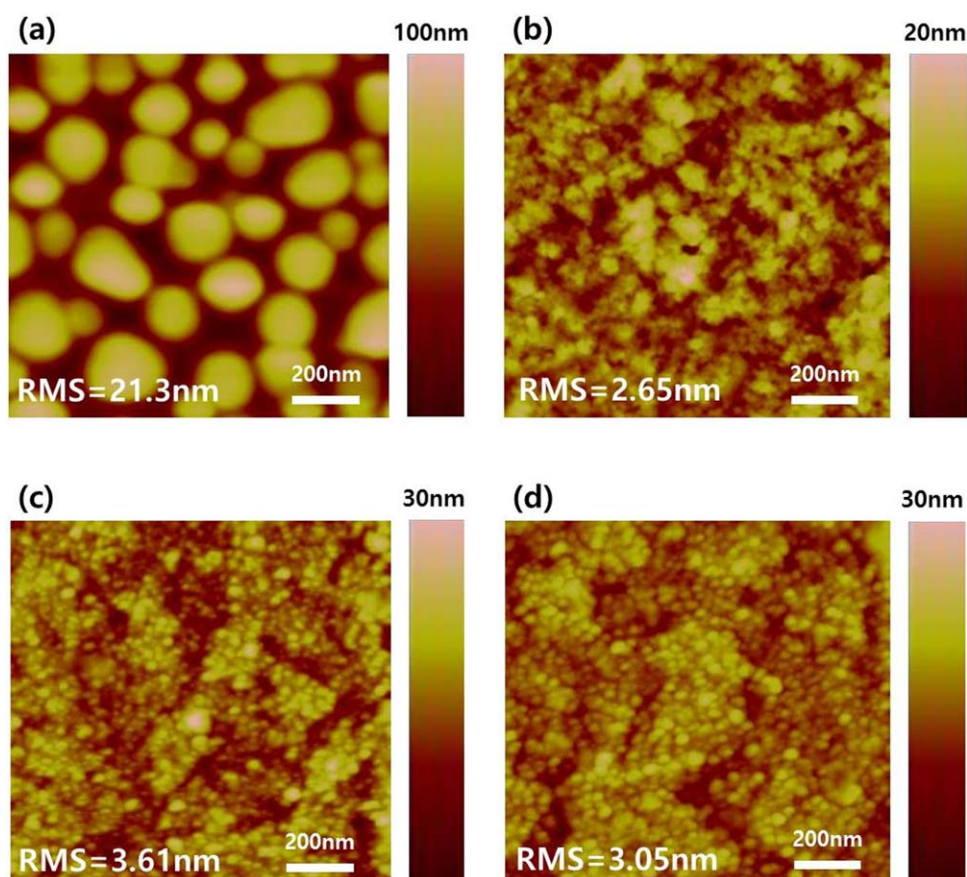


FIGURE 5 Tapping-mode AFM topography images of (a) PBBDT-tTz:PC₇₁BM (1.0:2.0), (b) PBBDT-tTz:PC₇₁BM (1.0:2.0), (c) PBBDT-tTz:PC₇₁BM (1.0:2.0 with 1 vol % 1-CN), and (d) PBBDT-ttTz:PC₇₁BM (1.0:2.0 with 1 vol % 1-CN) blend films. [Color figure can be viewed at wileyonlinelibrary.com]

and sulfur atom of the BDT unit led to distortion in the polymer and a dihedral angle of 25°. The replacement of π -bridges from the thiophene units to thieno[3,2-*b*]thiophene units resulted in a change in the backbone conformation of the polymer from zigzagged to a linear conformation. Even though PBBDT-ttTz had a dihedral angle of 35° between BDT and thieno[3,2-*b*]thiophene units, it adopted a linear backbone conformation as a result of the parallel bonds on the 2- and 5-positions of thieno[3,2-*b*]thiophene. The thieno[3,2-*b*]thiophene π -bridge favored the linear backbone conformation in this case because both BDT and Tz are linear linkers. The HOMOs of the two polymers were delocalized along their entire backbones, while the LUMOs were largely localized on the electron accepting Tz unit.

Photovoltaic Performances and Hole Mobilities

To investigate the photovoltaic performances of PBBDT-tTz and PBBDT-ttTz, BHJ OPV devices were fabricated with an inverted configuration of ITO/ZnO/polymer:PC₇₁BM/MoO₃/Ag. The weight ratios of polymer:PC₇₁BM blend films were varied as 1.0:1.0, 1.0:1.5, 1.0:2.0, and 1.0:3.0 to optimize the morphologies of the active layer. PC₇₁BM was selected as the electron acceptor because of its higher absorption coefficient in the visible region compared with that of PC₆₁BM, which is

a consequence of its distorted structure.³⁰ The *J-V* curves of the OPV devices fabricated with the different polymer:PC₇₁BM blend weight ratios are shown in Supporting Information Figure S3. As shown in Table 3, the optimized weight ratio for both PBBDT-tTz and PBBDT-ttTz in the polymer:PC₇₁BM blend, that is, at which the best photovoltaic performances were achieved, was 1.0:2.0. The OPV devices exhibited maximum PCE values of 1.50% and 5.21% for PBBDT-tTz and PBBDT-ttTz, respectively. PBBDT-ttTz showed similar *V*_{OC} but higher *J*_{SC} and *FF* values compared with those of PBBDT-tTz [Fig. 4(a,b)]. Additionally, PBBDT-ttTz had a higher EQE than PBBDT-tTz in the range of 350–600 nm [Fig. 4(c)]. The PBBDT-ttTz-based device showed an excellent *J*_{SC} value that exceeded 10 mA/cm² and an *FF* of approximately 65%. The *J*_{SC} values are affected by many factors including the absorption properties, charge carrier mobility, morphology, and crystallinity of the blend layer.^{1,24} The higher *J*_{SC} of the PBBDT-ttTz-based device compared with that of the PBBDT-tTz-based device was likely a result of the different polymer crystallinities arising due to the introduction of thieno[3,2-*b*]thiophene π -bridges, which affected the charge carrier mobility and p-n heterojunction morphology of the active layer. Interestingly, addition of 1 vol % chloronaphthalene (1-CN) as a processing additive to the polymer:PC₇₁BM

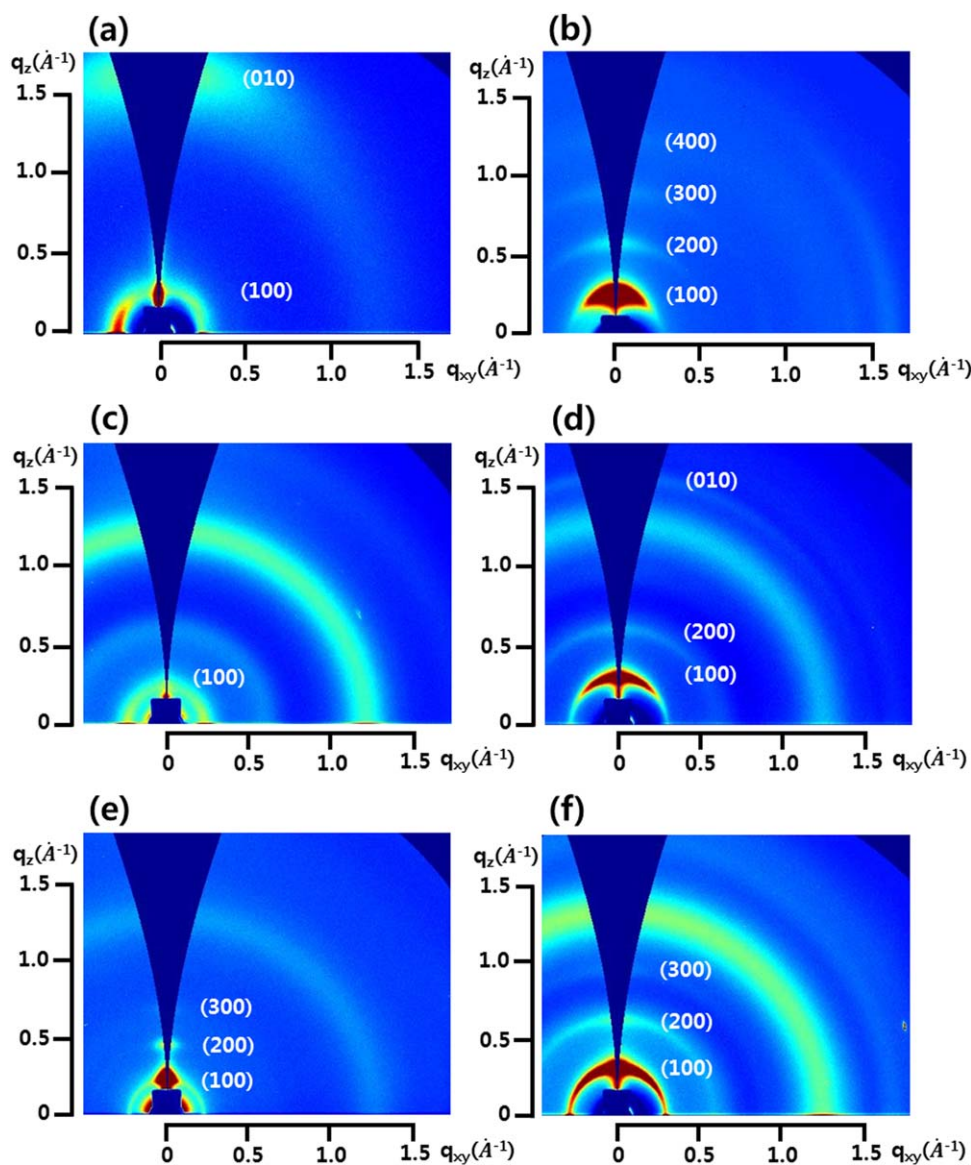


FIGURE 6 2D GIWAXS patterns of (a) PBBDT-tTz, (b) PBBDT-ttTz, (c) PBBDT-tTz:PC71BM (1.0:2.0, w/w), (d) PBBDT-ttTz:PC71BM (1.0:2.0, w/w), (e) PBBDT-tTz:PC71BM (1.0:2.0, w/w, 1 vol % 1-CN), and (f) PBBDT-ttTz:PC71BM (1.0:2.0, w/w, 1 vol % 1-CN) blend films. [Color figure can be viewed at wileyonlinelibrary.com]

blends affected the PBBDT-tTz- and PBBDT-ttTz-based devices differently. The PBBDT-tTz-based device showed an improvement in all parameters such as V_{OC} , J_{SC} , FF , and EQE , and consequently the PCE was increased from 1.50% to 2.92% (Fig. 4). On the contrary, the PBBDT-ttTz-based device showed a decrease in J_{SC} , FF , and EQE values, and the PCE was reduced from 5.21% to 3.99% upon addition of the additive in the blend film. The effect of the additive is discussed in more detail in the film morphology section.

The hole mobilities of the polymer:PC₇₁BM (1.0:2.0) blend films were 2.21×10^{-4} cm²/V-s and 9.61×10^{-4} cm²/V-s for PBBDT-tTz and PBBDT-ttTz, respectively (Table 3). The latter blend film showed a higher hole mobility than the former, resulting in a higher J_{SC} value because of the reduced degree

of recombination processes between holes and electrons.³¹ The hole mobilities of the polymer:PC₇₁BM blend films with 1-CN additives were 5.04×10^{-4} cm²/V-s and 7.07×10^{-4} cm²/V-s for PBBDT-tTz and PBBDT-ttTz, respectively. While the hole mobility of the PBBDT-tTz:PC₇₁BM blend film was increased, that of the PBBDT-ttTz:PC₇₁BM blend film was decreased upon addition of 1-CN. This indicated that the 1-CN additive impeded charge-carrier mobility in the PBBDT-ttTz blend film.

Film Morphologies

Tapping-mode atomic force microscope (AFM) was used to investigate the film surface morphology of the polymers according to their structures. AFM topography images of the polymer:PC₇₁BM blend films are shown in Figure 5. As

shown in Figure 5(a,b), the PBDT-tTz:PC₇₁BM blend film exhibited a smaller domain size and a smoother surface than the PBDT-tTz:PC₇₁BM blend film. The uniform and bi-continuous network of the PBDT-tTz:PC₇₁BM blend implied good miscibility between PBDT-tTz and PC₇₁BM. This contributed to an efficient charge separation and transport in the active layer, and consequently the PBDT-tTz:PC₇₁BM blend film could achieve a high J_{SC} value. However, the PBDT-tTz:PC₇₁BM blend film exhibited a rough surface and a high root-mean-square (RMS) roughness value over 20 nm impeding smooth current flow. As shown in Figure 5(c,d), the PBDT-tTz:PC₇₁BM blend film with the additive showed a remarkable improvement in morphology, while the PBDT-tTz:PC₇₁BM blend film with the additive showed an increased roughness of film surface.

To gain a deeper understanding of the characteristics of the polymer nanostructures in the blend films including crystal-orientation, crystal coherence length, and intermolecular distance, GIWAXS measurements were performed on pristine and blend films.²⁴ The 2D-GIWAXS patterns and 1D out-of-plane plots of all films are shown in Figure 6 and Supporting Information Figure S5, respectively. The PBDT-tTz pristine film showed a face-on orientation in the out-of-plane direction with a strong (010) reflection peak at $q_z = 1.60 \text{ \AA}^{-1}$ ($d_{(010)} = 3.93 \text{ \AA}$) while the pristine PBDT-tTz film showed an edge-on orientation with (100), (200), (300), and (400) reflection peaks with high crystallinity [Fig. 6(a,b)]. The thieno[3,2-*b*]thiophene π -bridges in PBDT-tTz improved the crystallinity of the polymer in the solid thin film state as compared with thiophene π -bridges in PBDT-tTz. The strong (010) peak of the face-on structure of PBDT-tTz disappeared on blending with PC₇₁BM in the PBDT-tTz:PC₇₁BM blend film. This indicated that the PBDT-tTz film lost its crystallinity and adopted an amorphous-like orientation when it was blended with PC₇₁BM [Fig. 6(c)]. On the other hand, the PBDT-tTz:PC₇₁BM blend film showed a bimodal structure of edge-on orientations with (100) and (200) peaks and face-on orientation with the (010) reflection peak at $q_z = 1.58 \text{ \AA}^{-1}$ ($d_{(010)} = 3.98 \text{ \AA}$) [Fig. 6(d)]. PBDT-tTz conserved its crystallinity even though the original polymer orientation was partially changed from edge-on to face-on when it was blended with PC₇₁BM. The higher molecular ordering of the PBDT-tTz:PC₇₁BM blend film compared with that of PBDT-tTz:PC₇₁BM resulted in higher J_{SC} and FF values, and consequently higher PCE because of efficient charge-carrier transportation of holes and electrons.^{32,33} Furthermore, the partial face-on structure of PBDT-tTz:PC₇₁BM possibly helped to improve the OPV device performances.

Addition of 1 vol % 1-CN additive to the PBDT-tTz:PC₇₁BM blend film led to improved crystallinity of the components, as evident from the enhanced edge-on orientation of (100), (200), and (300) reflection peaks [Fig. 6(e)]. The enhanced J_{SC} value of the PBDT-tTz:PC₇₁BM blend film with 1-CN additive could be attributed to the improved molecular ordering and well-organized p-n heterojunction morphology of the active layer. In contrast, the PBDT-tTz:PC₇₁BM blend film

showed decreased polymer crystallinity upon addition of the 1-CN additive, as evidenced by the disappearing (010) peak [Fig. 6(f)]. The decreased molecular ordering of the polymer film affected the J_{SC} value and led to decreased OPV performances of the PBDT-tTz:PC₇₁BM blend film with 1-CN additive.

CONCLUSIONS

In this study, two new D- π -A type conjugated wide-band gap copolymers, PBDT-tTz and PBDT-tTz, were synthesized and BHJ organic photovoltaic cells with these two polymers as acceptor materials in the photoactive layers were fabricated. PBDT-tTz and PBDT-tTz showed different molecular ordering behavior in solid thin film state depending on the presence of either 4-alkyl thiophene or 6-alkyl thieno[3,2-*b*]thiophene π -bridges between the BDT and Tz units. PBDT-tTz, which possessed 6-alkyl thieno[3,2-*b*]thiophene π -bridges in the polymer, exhibited strong π - π molecular stacking even in the solution state owing to its linear molecular structure. The PBDT-tTz:PC₇₁BM (1.0:2.0, w/w) blend film showed higher crystallinity than the PBDT-tTz:PC₇₁BM (1.0:2.0, w/w) blend film, and consequently led to better OPV performances. The PBDT-tTz:PC₇₁BM blend film also showed a high PCE of 5.21% with a J_{SC} of 10.15 mA/cm², while the PBDT-tTz:PC₇₁BM blend film showed a relatively low PCE of 2.92% and a J_{SC} of 6.09 mA/cm². The PBDT-tTz-based film exhibited higher hole mobility and J_{SC} value because of attributes such as improved molecular ordering and well-organized p-n heterojunction morphology of the active layer as compared with the PBDT-tTz-based film.

ACKNOWLEDGMENTS

This work was supported by the R&D Convergence Program of NST (National Research Council of Science & Technology) of Republic of Korea (CAP-15-04-KITECH), and National Research Foundation (NRF) grants, funded by the Korean government (MSIT) (NRF-2017R1A2A2A05001345 and No. 2011-0030013 through GCRC SOP).

REFERENCES AND NOTES

- 1 J.-H. Kim, J. B. Park, I. H. Jung, A. C. Grimsdale, S. C. Yoon, H. Yang, D.-H. Hwang, *Energy Environ. Sci.* **2015**, *8*, 2352.
- 2 T. Liu, X. Pan, X. Meng, Y. Liu, D. Wei, W. Ma, L. Huo, X. Sun, T. H. Lee, M. Huang, H. Choi, J. Y. Kim, W. C. H. Choy, Y. Sun, *Adv. Mater.* **2017**, *29*, 1604251.
- 3 Y. Liu, J. Zhao, Z. Li, C. Mu, W. Ma, H. Hu, K. Jiang, H. Lin, H. Ade, H. Yan, *Nat. Commun.* **2014**, *5*, 5293.
- 4 J. Zhao, Y. Li, G. Yang, K. Jiang, H. Lin, H. Ade, W. Ma, H. Yan, *Nat. Energy.* **2016**, *1*, 15027.
- 5 J.-H. Kim, S. Wood, J. B. Park, J. Wade, M. Song, S. C. Yoon, I. H. Jung, J.-S. Kim, D.-H. Hwang, *Adv. Funct. Mater.* **2016**, *26*, 1668.
- 6 B. Guo, X. Guo, W. Li, X. Meng, W. Ma, M. Zhang, Y. Li, J. Mater. Chem. A **2016**, *4*, 13251.

- 7 J.-H. Kim, C. E. Song, H. U. Kim, I.-N. Kang, W. S. Shin, M.-J. Park, D.-H. Hwang, *Polym. Chem.* **2013**, *51*, 4136.
- 8 L. Huo, S. Zhang, X. Guo, F. Xu, Y. Li, J. Hou, *Angew. Chem. Int. Ed.* **2011**, *50*, 9697.
- 9 H. Yao, L. Ye, H. Zhang, S. Li, S. Zhang, J. Hou, *Chem. Rev.* **2016**, *116*, 7397.
- 10 J.-H. Kim, H. S. Kim, J. B. Park, I.-N. Kang, D.-H. Hwang, *Polym. Chem.* **2014**, *52*, 3608.
- 11 J. R. Johnson, D. H. Rotenberg, R. Ketcham, *J. Am. Chem. Soc.* **1970**, *92*, 4046.
- 12 Q. Q. Shi, H. J. Fan, Y. Liu, J. Chen, Z. Shuai, W. Hu, Y. Li, X. Zhan, *J. Polym. Sci. A* **2011**, *49*, 4875.
- 13 Q. Q. Shi, H. J. Fan, Y. Liu, W. P. Hu, Y. F. Li, X. W. Zhan, *J. Phys. Chem. C* **2010**, *114*, 16843.
- 14 M. Yang, B. Peng, B. Liu, Y. Zou, K. Zhou, Y. He, C. Pan, Y. Li, *J. Phys. Chem. C* **2010**, *114*, 17989.
- 15 M. Zhang, X. Guo, Y. Li, *Adv. Energy. Mater.* **2011**, *1*, 557.
- 16 I. H. Jung, Y. K. Jung, J. Lee, J.-H. Park, H. Y. Woo, J.-I. Lee, H. Y. Chu, H.-K. Shim, *Polym. Chem.* **2008**, *46*, 7148.
- 17 V. Sannasi, D. Jeyakumar, *Chem. Select.* **2017**, *2*, 1992.
- 18 I. Osaka, R. Zhang, G. Sauve, D. M. Smilgies, T. Kowalewski, R. D. McCullough, *J. Am. Chem. Soc.* **2009**, *131*, 2521.
- 19 I. Osaka, G. Sauve, R. Zhang, T. Kowalewski, R. D. McCullough, *Adv. Mater.* **2007**, *19*, 4160.
- 20 H. Bronstein, Z. Chen, R. S. Ashraf, W. Zhang, J. Du, J. R. Durrant, P. S. Tuladhar, K. Song, S. E. Watkins, Y. Geerts, M. M. Wienk, R. A. J. Janssen, T. Anthopoulos, H. Sirringhaus, M. Heeney, I. McCulloch, *J. Am. Chem. Soc.* **2011**, *133*, 3272.
- 21 X. Wang, Y. Sun, S. Chen, X. Guo, M. Zhang, X. Li, Y. Li, H. Wang, *Macromolecules* **2012**, *45*, 1208.
- 22 H. Hwang, D. H. Sin, C. Kulshreshtha, B. Moon, J. Son, J. Lee, H. G. Kim, J. Shin, T. Joo, K. Cho, *J. Mater. Chem. A* **2017**, *5*, 10269.
- 23 J. C. Speros, H. Martinez, B. D. Paulsen, S. P. White, A. D. Bonifas, P. C. Goff, C. D. Frisbie, M. A. Hillmyer, *Macromolecules* **2013**, *46*, 5184.
- 24 J.-H. Kim, J. B. Park, F. Xu, D. Kim, J. Kwak, A. C. Grimsdale, D.-H. Hwang, *Energy Environ. Sci.* **2014**, *7*, 4118.
- 25 A. E. Labban, J. Warnan, C. Cabanetos, O. Ratel, C. Tassone, M. F. Toney, P. M. Beaujuge, *ACS Appl. Mater. Interfaces* **2014**, *6*, 19477.
- 26 L. Chen, P. Shen, Z.-G. Zhang, Y. Li, *J. Mater. Chem. A* **2015**, *3*, 12005.
- 27 J.-H. Kim, J. B. Park, I. H. Jung, S. C. Yoon, J. Kwak, D.-H. Hwang, *J. Mater. Chem. C* **2015**, *3*, 4250.
- 28 C. Maglione, A. Carella, R. Centore, P. Chavez, P. Leveque, S. Fall, N. Leclerc, *Dyes Pigm.* **2017**, *141*, 169.
- 29 J.-H. Kim, J. B. Park, S. C. Yoon, I. H. Jung, D.-H. Hwang, *J. Mater. Chem. C* **2016**, *4*, 2170.
- 30 S.-J. Ko, W. Lee, H. Choi, B. Walker, S. Yum, S. Kim, T. J. Shin, H. Y. Woo, J. Y. Kim, *Adv. Energy Mater.* **2015**, *5*, 1401687.
- 31 M. L. Keshtov, D. V. Marochkin, V. S. Kochurov, A. R. Khokhlov, E. N. Koukaras, G. D. Sharma, *J. Mater. Chem. A* **2014**, *2*, 155.
- 32 H. Kim, B. Lim, H. Heo, G. Nam, H. Lee, J. Y. Lee, J. Lee, Y. Lee, *Chem. Mater.* **2017**, *29*, 4301.
- 33 I. H. Jung, J.-H. Kim, S. Y. Nam, C. Lee, D.-H. Hwang, S. C. Yoon, *J. Mater. Chem. C* **2016**, *4*, 663.